

# Preparation and Properties of Hybrid Cement-in-Polymer Coatings Used for the Improvement of Fiber-Matrix Adhesion in Textile Reinforced Concrete

Oliver Weichold

DWI an der RWTH Aachen e.V. und Institut für Technische und Makromolekulare Chemie der RWTH Aachen, Pauwelsstraße 8, D-52074, Aachen

Received 9 September 2009; accepted 12 November 2009

DOI 10.1002/app.31815

Published online 22 February 2010 in Wiley InterScience (www.interscience.wiley.com).

**ABSTRACT:** Reactive cement-in-polymer dispersions have been prepared from poly(vinyl alcohol), poly(ethylene-co-vinyl acetate), and poly(vinyl acetate) and a non-hydrated, fine-grained cement, and used to coat multifilament glass-rovings. The influence of the molecular properties of the polymer, such as the chemical composition and molecular weight as well as the cement content in the dispersion, on the reinforcing performance of the coated rovings in concrete has been studied using scanning electron microscopy and tensile tests. All coated rovings significantly surpass the uncoated glass in terms of

mechanical behavior. The best bonding was obtained with hydrophobic, PVAc-based coatings, since the slow hydrolysis and swelling of this polymer controls cement hydration and the formation of the interphase. The mechanical behavior of the coated rovings is barely influenced by the molecular weight of the polymer, but decreases with decreasing cement content. © 2010 Wiley Periodicals, Inc. *J Appl Polym Sci* 116: 3303–3309, 2010

**Key words:** coatings; electron microscopy; mechanical properties; reinforcement; compounding

## INTRODUCTION

Polymers are indispensable components in modern concrete.<sup>1</sup> They mainly serve two purposes, namely as rheological additives, so-called superplasticizers,<sup>2</sup> and as structural additives in polymer concrete or polymer-modified concrete, where they replace parts of the cement hydrate binder.<sup>3,4</sup> A great number of polymers have been studied as structural additives, including liquid epoxy resins,<sup>5,6</sup> redispersible powders,<sup>7–9</sup> and polymer lattices.<sup>10,11</sup> Of particular interest are water-soluble polymers such as poly(vinyl alcohol) (PVA), which are simply added to the mixing water. This causes an increase in the aggregate-paste bond strength,<sup>12</sup> and a 60–80% increase in the pull-out load and frictional bond strength for steel and brass fibers.<sup>8</sup> This was explained by a modification of the interfacial structure, as evidenced by the formation of a dense, finely grained, and ductile structure in place of the usual calcium hydroxide–calcium silicate hydrate duplex layer.<sup>14</sup> A direct interaction between PVA and calcium ions in the

cement paste as well as in calcium silicate hydrate was subsequently corroborated.<sup>15–17</sup>

We have recently introduced another type of application for polymers in concrete, namely as part of reactive coatings for reinforcements. Based on the reported beneficial effects of PVA in cement paste, we developed a water-free cement-in-PVA dispersion as a coating for multifilament glass-rovings, to be used as reinforcement in textile-reinforced concrete.<sup>18</sup> The performance of multifilament rovings largely depends on how well the filaments are embedded in concrete.<sup>19</sup> Rovings contain several hundreds of individual filaments of 10–30  $\mu\text{m}$  in diameter, held together by a sizing agent. Adhesive forces between the individual filaments and other surface properties of the filaments can obstruct the ingress of the viscous, high-solid dispersion of the cement paste. This leads to a highly inhomogeneous roving penetration and the differentiation of outer and inner filaments, i.e., those that are in contact with the cement matrix (the outer ones) and others which are not (the inner ones).<sup>20,21</sup> Load transfer from the matrix to the inner filaments is only accomplished by adhesive cross-linkages<sup>22</sup> and friction, and in this way the inner filaments contribute less to the load-bearing capacity.<sup>20,21</sup>

By using a cement-in-PVA dispersion, containing nonhydrated cement particles, as coating for the roving, reactive cement particles are placed between the individual filaments before the roving gets into

Correspondence to: O. Weichold (weichold@dw.rwth-aachen.de).

Contract grant sponsor: Deutsche Forschungsgemeinschaft; contract grant number: SFB 532.

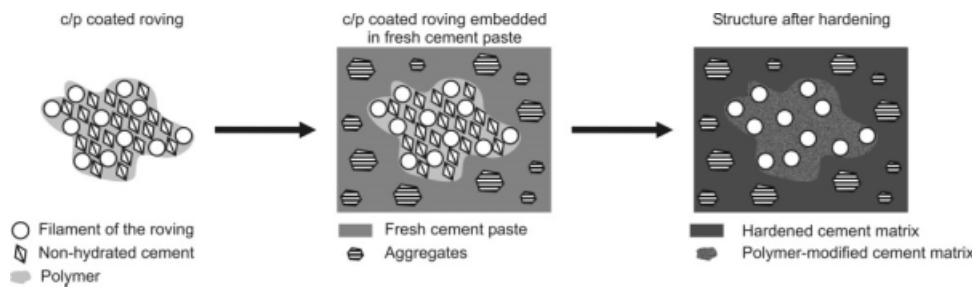


**Figure 1** Schematic illustration of the phase composition during embedding and hardening of glass rovings coated with cement-in-polymer dispersions.

contact with the aqueous cement paste. Thus, roving penetration no longer depends on the ingress of the cement paste. Upon embedding in fresh concrete, the polymer dissolves and the nonhydrated cement particles between the filaments are exposed to the aqueous environment of the cement paste. This enables the formation of a continuous matrix between the filaments (Fig. 1). As a result, improved bonding and an increase in the pull-out load was observed.

Herein we present a detailed study on the preparation and properties of cement-in-polymer dispersions (c/p) and on the influence of the polymer on the performance of rovings coated with cement-in-polymer dispersions. The chemical properties of the polymers, namely PVA, poly(ethylene-co-vinyl acetate) (EVA), and poly(vinyl acetate), are used to control the diffusion of moisture into and through the polymer phase. This provides the means to control the formation of the interfacial transition zone and, thus, the macroscopic behavior of the composite.

## EXPERIMENTAL

### Materials

PVA,  $M_w = 9500$ , saponification number 302, and poly(vinyl acetate)s, PVAc,  $M_w = 110,000$ – $150,000$  and  $M_w = 330,000$ – $430,000$ , were from Wacker. Poly(vinyl acetate),  $M_w = 55,000$ – $70,000$  was obtained from Roth. EVA,  $M_w = 110,000$  and with a vinyl acetate content of 40%, was obtained from Aldrich. Mikrodur P-X, Dyckerhoff, Neuwied, with a  $d_{95} < 6 \mu\text{m}$  was used to prepare the hybrid cement-in-polymer coatings. A Portland cement matrix designated PZ-0899-01 (water-to-binder ratio = 0.4) was used to prepare the pull-out specimen. Details on composition and properties can be found in Ref. 23 Continuous alkali-resistant glass-rovings (CEM-Fil® LTR ARC 2400 5325, 2400 tex, roving cross-section  $0.896 \text{ mm}^2$ , filament diameter  $27 \mu\text{m}$ ) were purchased from OCV Reinforcements.

### Methods

The cement-in-polymer dispersions were prepared by first dissolving the polymer in an appropriate amount of THF (PVA) or ethyl acetate (EVA, PVAc) and then adding the calculated amount of cement to obtain the desired cement content  $w = m_{\text{cement}} / (m_{\text{cement}} + m_{\text{polymer}})$ . The mixtures were used immediately, but can be stored in a tightly sealed container for months. During this time, most of the cement sediments, but vigorous stirring for 30 min restores the original quality. For coating, the roving is passed through a trough filled with the coating formulation followed by a  $0.5 \times 5 \text{ mm}$  die. The coated strands are allowed to dry in a hood over night. In the dry state the applied coating accounts for  $\sim 40 \text{ wt } \%$  of the total weight of the coated roving.

Load-displacement ( $P$ - $d$ ) curves for both tensile-strength tests and double-sided pull-out tests were recorded on a Zwick 1425 tensile-testing machine as described previously.<sup>18,24</sup> The SEM images were recorded on a Hitachi S-3000N with an Ametek EDAX.

## RESULTS AND DISCUSSION

### Preparation

The incorporation of nonhydrated cement clinker into water and/or alkali soluble polymers gives rise to reactive cement-in-polymer dispersions abbreviated as c/p in analogy to the abbreviation of e.g., water-in-oil (w/o) emulsions. The polymers used for these dispersions are shown in Figure 2. The degree of hydrolysis and the molecular weight of the PVA were chosen in such a way that the polymer dissolves readily in the cement paste at ambient temperature, can be processed thermoplastically, and can be homogeneously dispersed in THF. High cement contents of  $w > 0.9$  can be realized in the c/p dispersions with all polymers, since the viscosity of the coating formulations can be adjusted by the addition of solvents. However, such coatings are mechanically sensitive due to the low polymer

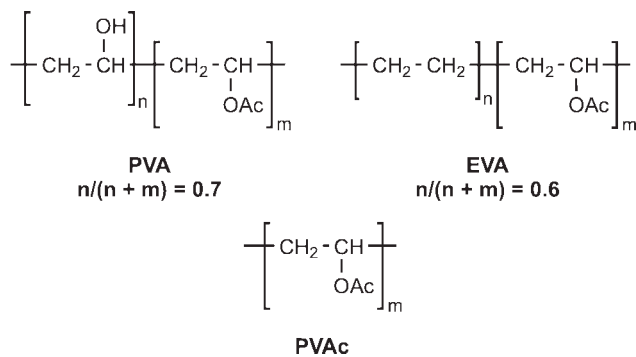


**Figure 2** Structures of the polymers used to prepare the c/p dispersions.

content. Therefore, coatings of  $w = 0.8$  are used as standard, which corresponds to more than 60 vol % of cement.

The pure c/PVAc mixtures can be prepared and processed thermoplastically up to  $w = 0.7$ , and c/PVA mixtures up to  $w = 0.6$  in standard laboratory kneaders and extruders [Fig. 3(A)].

For reasons of convenience, the c/p dispersions are prepared and applied on a lab scale from organic solvents. Because of the high solid content, all c/p-coated rovings under investigation are brittle and cannot be wound onto a bobbin. This also applies to the ones based on the thermoplastic elastomer EVA. However, gentle heating to approximately 35–40°C softens the polymer and the coated rovings can now be bent and spooled. Upon further heating to ~ 60°C the coated rovings can be fused under slight pressure. This allows for the preparation of inherently stable reinforcement grids or baskets in analogy to the currently used steel mats [Fig. 3(B)].

### Microscopic analysis

Microscopic analyses are shown for c/PVA [Fig. 4(A)] and c/PVAc [Fig. 4(B)] coated rovings ( $w =$

0.8), since these two polymers mark the two extremes in terms of polymer properties, with PVA being hydrophilic and water soluble, while PVAc is hydrophobic, and only soluble in alkaline solutions. Figure 4 shows polished cross-sections of specimen, which contain coated rovings, 7 days after being embedded in fresh concrete. In both cases, the filaments are to a large extent individually embedded and surrounded by a cementitious matrix, but both images show voids inside the roving (black areas). These are artifacts from the lab-scale, solvent-based coating process. Evaporation of the solvent causes the polymer phase to shrink, leaving behind the observed voids. Combined thermal annealing/compacting of the coated rovings, similar to the fusion procedure described earlier, reduces the internal cavities.

The c/PVA coated rovings exhibit two matrix zones [Fig. 4(A)], namely the dense bulk matrix (i) outside and a darker phase inside the roving interspersed with voids (ii). The latter constitutes the hydrated c/p phase and appears darker in the back-scattering mode of the SEM, due to its lower density. At the transition from (i) to (ii), filaments are individually embedded in the bulk matrix, which indicates a complete dissolution of the outer c/PVA coating followed by cocrystallisation of both coating components, cement and PVA, with the cement paste. In contrast, the c/PVAc coated roving shows a clear-cut boundary at the transition to the outer bulk matrix, while the inner c/p phase appears to have a granular texture [Fig. 4(B)].

The differences between these two polymers are reflected even better in the structure of the interface directly at the filament. Figure 5(A) shows a single filament extracted from a c/PVA coated roving embedded in concrete. The surface is overgrown with crystalline materials in some areas, mostly calcium hydroxide, and is totally bare in others indicating adhesive failure of the fiber/matrix interface. Under the same conditions, filaments in c/PVAc coated

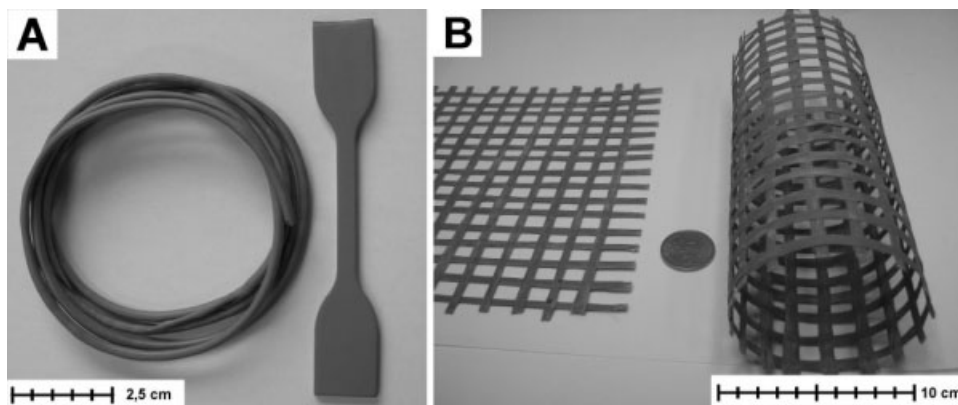


**Figure 3** Pure c/PVA dispersion at  $w = 0.6$ , extruded and injection molded (A) and fused nonwoven reinforcements made from ARG 2400 rovings coated with c/PVAc ( $w = 0.8$ ) (B).

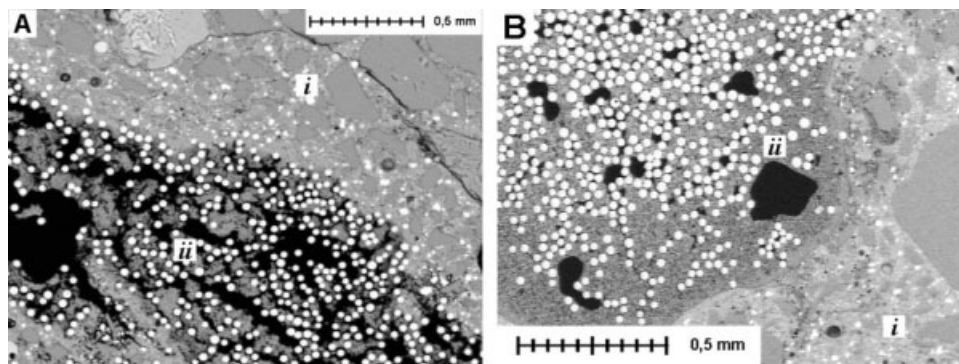


**Figure 4** Polished cross sections of concrete-embedded rovings. (A) c/PVA ( $w = 0.8$ , compare Table I, entry 3) and (B) c/PVAc ( $w = 0.8$ , compare Table I, entry 6). The black regions inside the roving indicate the voids.

rovings are embedded in a granular structure, consisting of partially-hydrated clinker crystals, and the remnants of crystalline material on the filaments indicate cohesive failure inside the interphase [Fig. 5(B)]. These differences in the interfacial structure can be attributed to the different dissolution rates of PVAc compared to PVA in alkaline solution. PVA dissolves readily within minutes in pore solution, thus, quickly exposing its cement content to the incoming aqueous cement paste. The space around the filaments is filled with cement paste, from which the excess  $\text{Ca}(\text{OH})_2$  crystallizes on the filament surface. In contrast, PVAc in the original state is hydrophobic, and initially is only poorly wetted by the alkaline solution. Upon prolonged exposure the acetate groups are hydrolysed to OH groups, which renders the polymer increasingly hydrophilic. During hydrolysis, the polymer swells at a slow rate, thereby slowly absorbing traces of the pore solution. The amount of water absorbed by the coating during swelling is not sufficient to fully hydrate the clinker and reach saturation of  $\text{Ca}(\text{OH})_2$  and, consequently, a partially-hydrated clinker structure forms. Thus, the hydration of the cement in c/PVAc coatings and, therewith, the formation of the interfacial transition zone<sup>25</sup> becomes diffusion controlled.

SEM-EDX mappings of concrete-embedded, c/PVA coated rovings show differences in the composition of the outer and inner matrix phase (Fig. 6). The boundary is shown as a dashed line in Figure 6(A). Along this border, the silicon distribution [Fig. 6(B)] indicates a transition from a Si-rich outer phase (light gray) to a Si-poorer phase (darker gray) interspersed with filaments. A quantitative analysis of the pixel intensities in the image (255 = white) along the horizontal line in Figure 6(B) allows the clear identification of quartz (intensity > 120), filaments (80–100), bulk matrix (40–50), c/p phase (30–40), and cavities (<20). In addition, the exact position of the c/p to bulk-matrix transition can be identified by an average increase of 20 gray-scale units [Fig. 6(C)]. Such a transition is not visible in the calcium mapping [Fig. 6(D)]. Therefore, while calcium seems to be distributed homogeneously within the sample, silicon is preferentially located in the bulk phase. This indicates free diffusion of calcium ions from the bulk matrix, which leads to an excess of  $\text{Ca}^{2+}$  in the c/p phase and explains the fast growth of calcium hydroxide on the filaments of c/PVA coated rovings [compare Fig. 6(A)]. The light gray spots in Figure 6(D) earmark the nonhydrated clinker in the bulk phase, something which is hardly found in the c/p

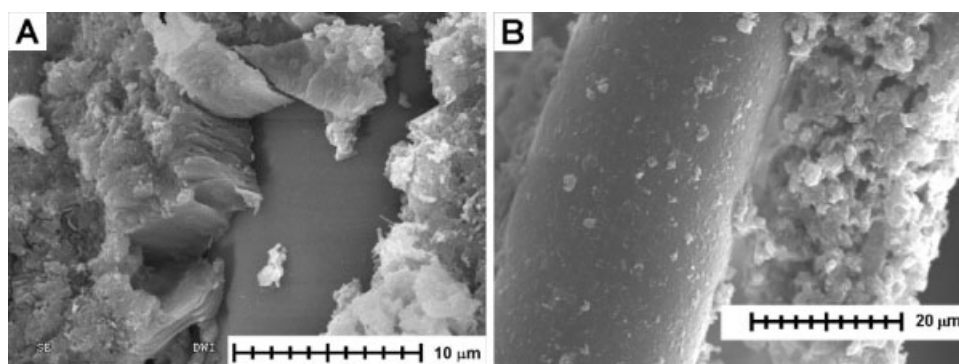


**Figure 5** Structure of the interfacial transition zone for c/PVA (A) and c/PVAc (B) coated rovings at  $w = 0.8$ . Samples were stored for 7d at 95% relative humidity.

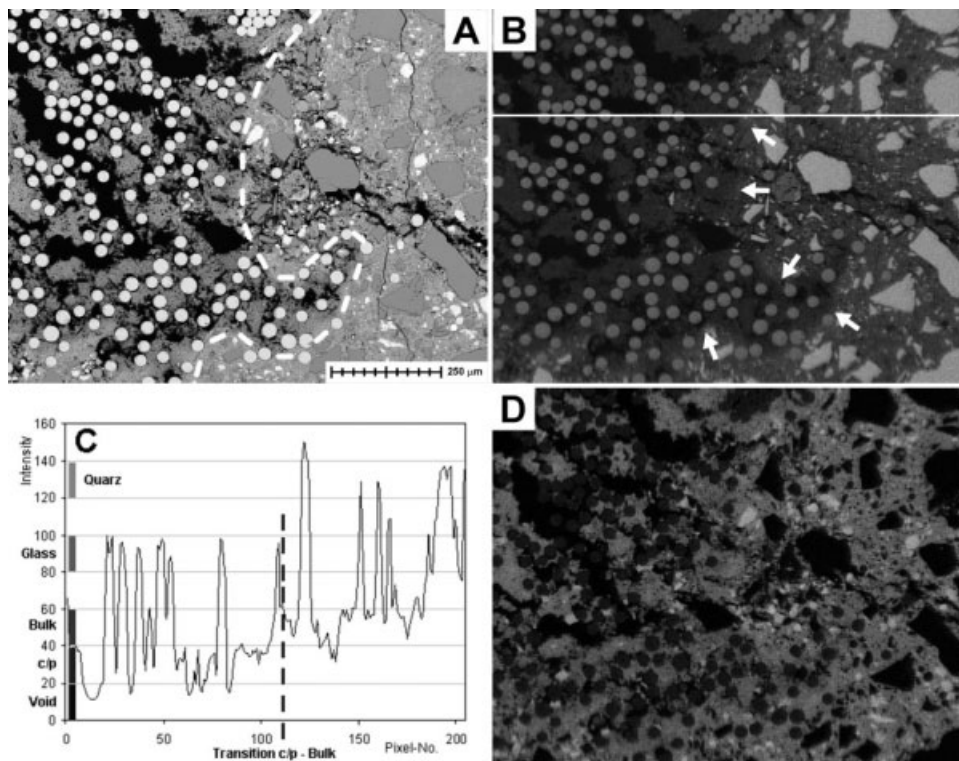


**Figure 6** SEM-EDX analysis of concrete-embedded c/PVA ( $w = 0.8$ ) coated rovings. (A) BS-SEM image, (B) elemental distribution of silicon, (C) quantitative analysis of the pixel intensities along the white line in B, and (D) elemental distribution of calcium.

phase, as this has a uniform, dark gray appearance. Since the c/p coating initially contained 80 wt % of clinker, this observation proves that in the case of the c/PVA coating, the pore solution completely penetrated the coating and reacted with the clinker as originally intended, to give a uniform polymer-modified cement-matrix between the filaments.

### Mechanical characterization

Figure 7 shows typical load-displacement curves of double-sided pull-out experiments for ARG2400 rovings coated with the c/p dispersions ( $w = 0.8$ ), in comparison to the as received roving (dashed line). Due to the occurrence of voids inside the c/p phase as a result of the lab-scale, solvent-based coating procedure (vide infra), no attempt was made to quantify the interfacial bonding. Rather, the measured load-displacement curves, and the values extracted from these, are compared as they are, under the assumption that a more perfect coating would give rise to higher pull-out loads.

All curves exhibit linear parts of similar slope in the ascending branch. The as received roving exhibits a low peak load  $P_{\text{peak,DPO}}$  and a drop to less than 20% of  $P_{\text{peak,DPO}}$  after passing the maximum, as a result of the filaments being pulled out of the con-

crete with little friction. Coating the roving with c/p dispersions significantly increases the peak loads and the load levels in the slippage regime. In the ascending branch, fiber debonding occurs up to  $P_{\text{peak,DPO}}$ , where the filaments are fully debonded. The lower  $P_{\text{peak,DPO}}$  values for c/PVA might be caused by two factors: (i) a lower degree of penetration of the c/PVA rovings, i.e., less filaments are

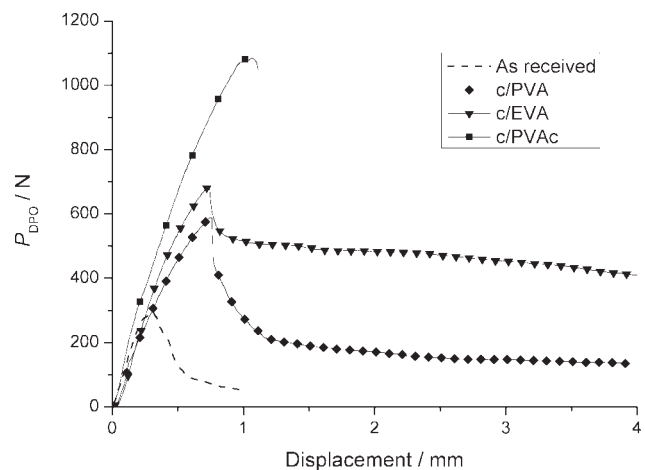


**Figure 7** Load-displacement curves of ARG 2400 rovings coated with c/p dispersions based on the three polymers under investigation.

TABLE I  
Mechanical Test of as Received and Coated ARG 2400 Rovings<sup>a</sup>

Entry	Coating	Test <sup>b</sup>	$P_{\text{peak}}$ N	$\phi^c$	$W_{\text{peak}}$ (mJ)	$W_{2\text{mm}}$ (mJ)
1	–	TST	886 ± 47	<i>0.34 ± 0.09</i>	<i>59 ± 11</i>	–
2	–	DPO	300 ± 39			
3	c/PVA, $w = 0.8$	DPO	599 ± 38	<i>0.68 ± 0.06</i>	<i>246 ± 43</i>	<i>575 ± 55</i>
4	c/EVA, $w = 0.8$	DPO	657 ± 85	<i>0.74 ± 0.10</i>	<i>297 ± 97</i>	<i>923 ± 145</i>
5	c/PVAc, $w = 0.8$ , $M_w = 55,000$	DPO	1083 ± 65	<i>1.22 ± 0.10</i>	<i>702 ± 90</i>	–
6	c/PVAc, $w = 0.8$ , $M_w = 110,000$	DPO	1118 ± 78	<i>1.26 ± 0.11</i>	<i>730 ± 154</i>	–
7	c/PVAc, $w = 0.8$ , $M_w = 330,000$	DPO	933 ± 50	<i>1.05 ± 0.08</i>	<i>525 ± 75</i>	<i>1290 ± 89</i>

<sup>a</sup> Measured values are given in roman type, values calculated from these are given in italic type.

<sup>b</sup> TST = tensile-strength test; DPO = double-sided pull-out.

<sup>c</sup> Ratio of pull-out load to tensile strength  $P_{\text{peak,DPO}}/P_{\text{peak,TST}}$ .

bound to the cement matrix, or (ii) a weaker interface due to the crystallization of soft  $\text{Ca}(\text{OH})_2$  on the filament surface. The microscopic analyses support a combination of both factors [compare Figs. 4(A) and 5(A)]. Similar to the as-received roving, the load-displacement curves for c/EVA (▼) and c/PVA (◆) show a pronounced drop of the load level at the onset of slippage when the maximum is passed. In contrast, pull-out is not observed with c/PVAc (■) coated rovings as the interfacial bond-strength exceeds the tensile strength of the roving, which is severed after passing  $P_{\text{peak}}$ .

Table I shows data extracted from the load-displacement curves. The reinforcing efficacy  $\phi = P_{\text{peak,DPO}}/P_{\text{peak,TST}}$ , with  $P_{\text{peak,TST}}$  being the tensile strength of the as received ARG2400 (entry 1), indicates how effective the strength of the glass roving is when used in pull-out experiments.<sup>18</sup> In the set of materials under investigation,  $\phi$  increases in the order ARG2400 < c/PVA80:20 < c/EVA80:20 < c/PVAc80:20 (entries 1–5) and, consequently, the c/PVAc coating is used for further studies.

To investigate the effect of the molecular weight on the pull-out performance, three PVAc samples with  $M_w = 55,000$ – $70,000$  (entry 5),  $110,000$ – $150,000$  (entry 6), and  $330,000$ – $430,000$  (entry 7), were used to prepare c/PVAc coatings of  $w = 0.8$ . Although for polymers with identical chemical composition, the chain mobility, rate of swelling, and the solubility decrease with increasing molecular weight, no significant influence of the molecular weight on the pull-out results was found (entries 5–7). This leads to the conclusion that cement hydration rather than diffusion of moisture is the rate determining step in the formation of the interfacial transition zone. For all three molecular weights, efficacies of larger than 1 were found (entries 5–7), i.e., the measured pull-out load exceeds the tensile strength of the roving. This is possible since rovings always contain a certain number of filament breaks.<sup>26</sup> Apparently, after being embedded in concrete the matrix between the individual filaments, formed by hydrolysing polymer and cement of the c/PVAc coating, is strong

enough to bridge some of the filament breaks and, thus, to push the failure load towards the theoretical value.

For all coated rovings, large values for the pull-out work  $W_{\text{peak}}$ , which represents the dissipated bond energy,<sup>27</sup> are observed. After passing  $P_{\text{peak}}$ , roving pull-out occurs at varying load-levels except for entries 5 and 6, where the filaments are severed. The pull-out leads to high values for  $W$  in the descending branch, with the friction largely contributing to the total pull-out work as documented by  $W_{2\text{mm}}$ .<sup>13</sup> This is especially pronounced for entry 7, for which pull-out occurs at  $\sim 800$  N.

To study the influence of the cement content  $w$  on the fiber-matrix adhesion, c/PVAc mixtures with  $w < 0.8$  have been investigated (Fig. 8), due to their superior thermoplastic processability. Upon decreasing  $w$ ,  $P_{\text{peak}}$  decreases from  $1118\text{N} \pm 78\text{N}$  at  $w = 0.8$  to  $456\text{N} \pm 62\text{N}$  at  $w = 0$  (pure PVAc), which still exceeds the value for the as received roving by 50%. Additionally, roving pull-out occurs at  $w < 0.8$ . The drop after passing from  $P_{\text{peak,DPO}}$  to the load level of the slippage regime increases with decreasing  $w$ , indicating a lower contribution of friction due to the

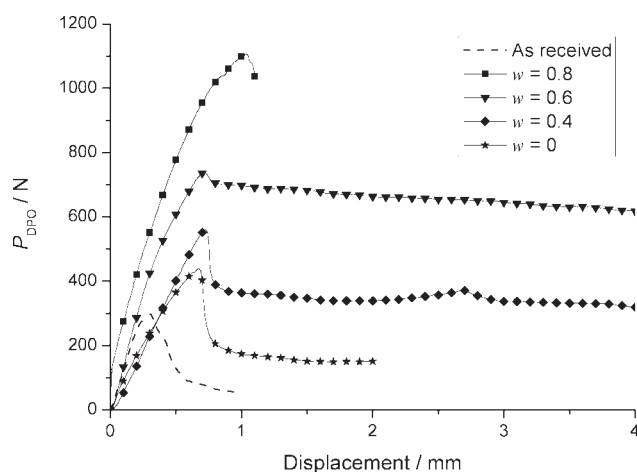


Figure 8 Load-displacement curves of c/PVAc coated ARG 2400 rovings at different cement content.

larger amount of polymer in the coating acting as lubricant, thus, giving rise to a softer interface.

### CONCLUSIONS

Uncoated glass rovings have severe shortcomings when used as reinforcements in concrete. We have developed a reactive coating consisting of a soluble polymer and nonhydrated cement, with which the pull-out loads can be increased four times and the dissipated bond energies up to 12 times, provided that the chemistry of the reactive components is properly adjusted. The rate of swelling and dissolving of the polymer directly controls the hydration of the cement and, thus, the formation of the interfacial transition zone between the filaments and the bulk matrix. As a consequence, the pull-out responses such as peak load and the frictional bond-strength in the slippage regime can be tuned via the polymer chemistry. The results demonstrate the high potential of glass rovings with engineered interphase as reinforcements to improve the macroscopic load-bearing behavior. This opens up new possibilities for the construction of light, but nonetheless stable construction elements made of concrete, thus, making previously unprecedented architectural parts possible.

The author thanks Dyckerhoff AG, Neuwied, for providing Mikrodur P-X and Wacker GmbH & Co KG, Burghausen, for the PVA and PVAc samples. He also thanks the technical assistance of Markus Hojczyk and Franz-Josef Steffens.

### References

1. Chung, D. D. L. *J Mater Sci* 2004, 39, 2973.
2. Mollah, M. Y. A.; Adams, W. J.; Schennach, R.; Cocke, D. L. *Adv Cem Res* 2000, 12, 153.
3. Ohama, Y. *Adv Cem Based Mater* 1997, 5, 31.
4. Van Gemert, D.; Czarnecki, L.; Maultzsch, M.; Schorn, H.; Beeldens, A.; Łukowski, P.; Knapen, E. *Cem Concr Compos* 2005, 27, 926.
5. Aggarwal, L. K.; Thapliyal, P. C.; Karade, S. R. *Construct Building Mater* 2007, 21, 379.
6. Abdel-Fattah, H.; El-Hawary, M. M. *Construct Building Mater* 1999, 13, 253.
7. Ci, X. H.; Falconio, R. R. *Cem Concr Aggregates* 1995, 17, 218.
8. Bright, R. P. *Cem Concr Aggregates* 1995, 17, 227.
9. Schneider, S. I.; Dewacker, D. R.; Palmer, J. G. In *Polymer-Modified Hydraulic-Cement Mixtures*, Kuhlmann, L. A., Walters, D. G., Eds.; American Society for Testing and Materials: Philadelphia, 1993, pp 76–89.
10. Won, J.-P.; Kim, J.-H.; Park, C.-G.; Kang, J.-W.; Kim, H.-Y. *J Appl Polym Sci* 2009, 112, 2229–2234.
11. Sumathy, C. T.; Dharakumar, M.; Devi, M. S.; Saccubai, S. *J Appl Polym Sci* 1997, 63, 1251–1257.
12. Kim, J.-H.; Robertson, R. E. *Adv Cem Based Mater* 1998, 8, 66.
13. Najm, H.; Naaman, A. E.; Chu, T. J.; Robertson, R. E. *Adv Cem Based Mater* 1994, 1, 115.
14. Chu, T. J.; Robertson, R. E.; Najm, H.; Naaman, A. E. *Adv Cem Based Mater* 1994, 1, 122.
15. Matsuyama, H.; Young, J. F. *Chem Mater* 1999, 11, 16.
16. Bonapasta, A. A.; Buda, F.; Colombet, P.; Guerrini, G. *Chem Mater* 2002, 14, 1016.
17. Di Maggio, R.; Della Volpa, C.; Gialanella, S.; Guerrini, G. *Chem Mater* 2001, 13, 4335.
18. Weichold, O.; Möller, M. *Adv Eng Mater* 2007, 9, 712.
19. Weichold, O.; Hojczyk, M. *Text Res J* 2009, 79, 1438.
20. Hegger, J.; Will, N.; Bruckermann O.; Voss, S. *Mater Struct* 2006, 39, 765.
21. Peled, A.; Zaguri, E.; Marom, G. *Compos A* 2008, 39, 930.
22. Schorn, H. *Bautechnik* 2003, 80, 174.
23. Brockmann, T. Ph.D. Thesis, RWTH, Aachen, 2005.
24. Raupach, M.; Brockmann, J. In *Proceedings of the CCC 2001*; Porto, 2001; pp 293–297.
25. Bentur, A.; Diamond, S.; Mindess, S. *J Mater Sci* 1985, 20, 3610.
26. Schmitz, G. K.; Metcalfe, A. G. *Mater Res Stand* 1967, 7, 146.
27. Alwan, J. M.; Naaman, A. E.; Hansen, W. *Cem Concrete Compos* 1991, 13, 247.